

Socioeconomic Drivers of Physical Morbidity Across U.S. Counties: A Spatial Causal Inference Approach

Ranadeep Daw^{1*}, Hunter Evans¹ and Indrabati Bhattacharya²

^{1*}Department of Mathematics and Statistics, University of West
Florida, 11000 University Pkwy, Pensacola, 32514, Florida, USA.

²Department of Statistics, Florida State University, 117 N. Woodward
Ave., Tallahassee, 32306, Florida, USA.

*Corresponding author(s). E-mail(s): rdaw@uwf.edu;
Contributing authors: hne8@students.uwf.edu; ib22g@fsu.edu;

Abstract

Identifying the causal effects of socioeconomic determinants on population health is of many great interests – from statistical methodology development to public health practitioners and policy developments. The statistical side of the problem needs to address several questions: spatial autocorrelation in both exposures and outcomes, confounding between treatments and covariates, and the need for geographically logical inference. We address these jointly by using spectral basis functions – Moran Eigenvector Maps and ICAR precision matrix eigenvectors – within a doubly robust generalized propensity score estimator for continuous treatments. Applied to 2022 county health data across the U.S. counties, the framework identifies the effect of six chosen predictors on the average physically unhealthy days per month. Possible further applications and methodological extensions are also discussed as future directions from this research.

Keywords: Physically unhealthy days, spatial statistics, basis functions, causal inference, doubly-robust estimator

1 Introduction

Population health outcomes in the United States exhibit striking geographic heterogeneity. Average physically and mentally unhealthy days, rates of chronic disease, and access to care vary substantially across counties. These patterns reflect the uneven geographic distribution of socioeconomic resources, environmental exposures, and structural disadvantage [1, 2] rather than chance. Understanding which of these factors drive poor health outcomes, and by how much, is essential for designing targeted public health interventions.

In this study, we focus on modeling average physically unhealthy days per month across U.S. counties as a function of socioeconomic and environmental determinants under a causal analysis framework. Causal estimation in this setting presents two key challenges. First, both the health outcomes and their predictors show strong spatial autocorrelation, and neighboring counties tend to resemble each other due to shared infrastructure and unmeasured local conditions. Ignoring this structure induces *spatial confounding*, which arises when latent geographic processes jointly influence both the treatment and the outcome [3, 4]. We need to decouple the treatment effects from the underlying spatial signal to quantify the effects of the predictors. Second, the exposures of interest in this paper – e.g., unemployment rate, food insecurity, etc. are continuous and hence necessitates the application of the *generalized propensity score* (GPS) [5, 6] framework, which extends the binary propensity-based causal inference methods to continuous exposure regimes by modeling the conditional and marginal densities of the treatment.

For causal inference, we employ a unified framework combining spatial basis function regularization and doubly robust GPS estimation. Spatial confounding is addressed by augmenting the regression with low-dimensional spectral basis functions derived from the county adjacency graph – specifically Moran Eigenvector Maps (MEM) and conditional autoregression (CAR/ICAR)-based basis functions [7, 8]. The basis function coefficients are regularized separately from the treatment effects to preserve causal interpretability. The GPS is then embedded in a doubly robust estimator [9], which is known to remain consistent if either the propensity or outcome model is correctly specified. Together, this approach aligns with the growing practice of (generalized) propensity score methods for casual analysis of spatially structured observational data [10, 11].

The remainder of the paper is organized as follows. Section 2 describes the data and reviews relevant methodological background. Section 3 presents the spatial causal inference methodology, including basis construction, GPS estimation, doubly robust estimation, and cross-fitting. Section 4 reports empirical results on basis function performance and causal effect estimates. Finally, Section 5 discusses implications, limitations, and directions for future work.

2 Data and Literature Review

Our analysis draws on county-level data over the U.S. counties and county-equivalents. The outcome variable – average physically unhealthy days per month – comes from the 2022 County Health Rankings & Roadmaps (CHR&R), derived from the CDC

Average Physically Unhealthy Days per Month
U.S. counties, 2022 County Health Rankings (BRFSS)

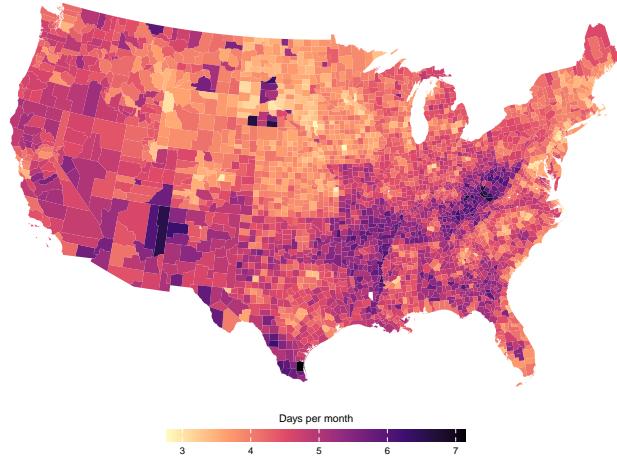


Fig. 1 Geographic distribution of average physically unhealthy days per month across U.S. counties (2022 County Health Rankings, derived from BRFSS). Darker shading indicates higher morbidity burden. Pronounced clustering in Appalachia, the Deep South, and parts of the rural Midwest motivates the spatial confounding adjustment central to our methodology.

Behavioral Risk Factor Surveillance System (BRFSS), and has been validated as a reliable proxy for population-level functional limitation and chronic disease burden [2]. Figure 1 shows the spatial distribution of the response variable, revealing a strong geographic pattern in physically unhealthy days across counties.

Predictor data are obtained in an analysis-ready format from the same CHR&R source, as well as from the American Community Survey (ACS) via `data.census.gov`. Figure 2 shows the spatial distribution of the six treatment variables considered in this study. Figure 2 shows the distribution of the six treatment variables that we have analyzed in this paper. All variables are measured at the county level, which serves as the unit of analysis for constructing the spatial adjacency graph underlying our basis functions. Related social determinant of health (SDOH) analyses in the literature include cross-sectional rankings [2], structural determinants frameworks [1], geographically weighted regression [12], and Bayesian spatiotemporal models [13] – though most of this work remains associative rather than causal.

Our goal here is to estimate the causal effects of the drivers on the average number of physically unhealthy days. As mentioned before, we need to account for the spatial dependence structure as well as decouple the effect of spatial confounding between the outcome and predictors arising from unmeasured geographic processes [4, 14, 15]. We address these questions through a dimension-reduction approach that constructs basis functions directly from the county neighborhood structure. Specifically, we explore two spectral bases (i.e., eigenvector-based basis functions) derived from the adjacency graph: Moran Eigenvector Maps (MEM) [16, 17] and eigenvectors from the (I)CAR precision matrix [18, 19], both of which parameterize the latent spatial surface via

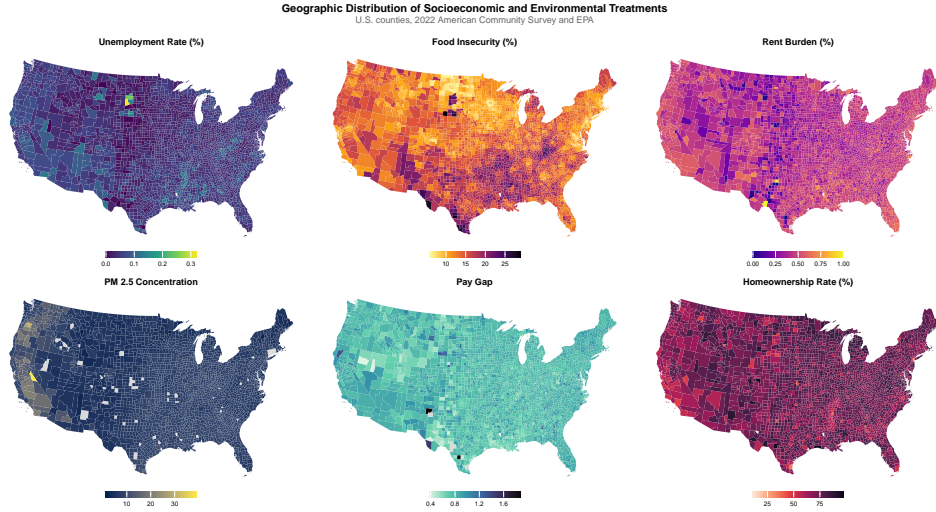


Fig. 2 Geographic distribution of the six socioeconomic and environmental treatments across U.S. counties. From left to right, top to bottom: unemployment rate, food insecurity, rent burden (American Community Survey, Table B25070), PM 2.5 concentration (EPA via CHR&R), pay gap, and homeownership rate. The visible spatial clustering across all six treatments illustrates why spatial confounding control is necessary prior to causal estimation.

leading eigenvectors of graph-derived operators. Causal estimation then proceeds via inverse probability weighting based on the generalized propensity score (GPS) [5, 20, 21], embedded within a doubly robust estimator [9, 22, 23]. Related recent work at this intersection includes Gao et al. [24], Papadogeorgou and Samanta [25], and Pollmann [26], among others.

3 Methodology

Our proposed framework is a combination of spectral dimension reduction for spatial basis function modeling at the first stage and subsequently applies a GPS-based doubly robust estimation for causal effect identification for such observational data. In below, we describe the technical details and the framework.

3.1 Data Structure and Assumptions

Suppose we have data over n counties indexed by $j = 1, \dots, n$. Let y_j denote the health outcome (average physically unhealthy days per month) for county j . Suppose that we are interested in modeling the outcome of the effect of m treatments denoted by $A_{\ell,j}$, where $\ell = 1, \dots, m$. Here we separately analyze the causal effect of $m = 6$ socioeconomic and environmental treatments: unemployment rate, food insecurity,

rent burden, income inequality, homeownership rate, and PM 2.5 concentration on the monthly average physically unhealthy days.

Let \mathbf{X}_j denote a set of additional socioeconomic covariates, including percentage of population aged 65+, percentage under 18, percentage of minority population (black, hispanic, and asian), percentage female, percentage rural, percentage of bachelor’s degree holders, median income, and percentage of uninsured adults. For the analysis of the treatment effect of A_ℓ , here we use \mathbf{X}_j as well as all the other treatments except the ℓ -th one (denoted by $\mathbf{A}_j^{-\ell}$) as confounders. Additionally, we denote $\mathbf{Z}_j \in \mathbb{R}^k$ as a set of spatial basis functions for county j , which we define in Section 3.2). Note that for the unemployment rate analysis, we exclude median income and percentage of uninsured adults from the confounding set.

Let $y(a_\ell)$ denote the potential outcome corresponding to treatment $A_\ell = A_{\ell,j}$; $\ell = 1, \dots, m$. Our objective in this article is to estimate the average treatment effect $\tau_\ell = \mathbb{E}[y(A_{\ell,j})]$ of each treatment. For causal identification, the following assumptions are required:

1. **Unconfoundedness (Conditional ignorability):** $y(A_{\ell,j}) \perp\!\!\!\perp A_{\ell,j} \mid \mathbf{X}, \mathbf{A}_j^{-\ell}, \mathbf{Z}$ for all $A_{\ell,j}$ in the support of $A_{\ell,j}$. Potential outcomes are independent of treatment assignment conditional on observed covariates and spatial basis. This states there is no unmeasured confounding after conditioning on \mathbf{X} and \mathbf{Z} .
2. **Overlap (Positivity):** $f(A_{\ell,j} \mid \mathbf{X}, \mathbf{A}_j^{-\ell}, \mathbf{Z}) > 0$ for all $(A_{\ell,j}, \mathbf{X}, \mathbf{A}_j^{-\ell}, \mathbf{Z})$ in the joint support, i.e., all covariate combinations have positive probability of receiving any treatment level. This ensures comparability across treatment values.
3. **Consistency (Well-defined interventions):** $A_{\ell,j} = A_{\ell,j} \implies y = y(A_{\ell,j})$. This means that the observed outcome under treatment $A_{\ell,j} = A_{\ell,j}$ equals the potential outcome under the current treatment $A_{\ell,j}$. This assumption requires no interference between units (SUTVA) and well-defined treatment effects.

Note that due to the spatial dependence nature of both the response and the predictor variables, it is usually desired to capture the geographic variation via some spatial analysis methodology. Here we use spatial basis functions, which we discuss in the next section. Following that, we will discuss the other components of the model.

3.2 Spatial Basis Construction

We control for spatial confounding via spectral decomposition of spatial connectivity graphs. Let $\mathbb{W} \in \{0, 1\}^{n \times n}$ denote the binary adjacency matrix where $w_{ij} = 1$ if counties i and j share either a boundary or a vertex (queen contiguity condition). We consider two spatial bases:

Moran Eigenvector Maps (MEM):

The MEM basis derives from the doubly-centered adjacency matrix:

$$\widetilde{\mathbb{W}} = \left(\mathbb{I} - \frac{\mathbf{1}\mathbf{1}^\top}{n} \right) \mathbb{W} \left(\mathbb{I} - \frac{\mathbf{1}\mathbf{1}^\top}{n} \right). \quad (1)$$

Eigenvectors of $\widetilde{\mathbb{W}}$ associated with the largest eigenvalues maximize Moran’s I statistic, and also isolate patterns of positive spatial autocorrelation [27]. We use the first k eigenvectors form $\mathbf{Z}_{\text{MEM}} \in \mathbb{R}^{n \times k}$ as the basis function design matrix for our problem.

ICAR Basis:

(Intrinsic) Conditional Autoregressive (ICAR) models specify spatial dependence via the graph Laplacian precision matrix $\mathbb{Q} = \mathbb{D} - \rho\mathbb{W}$, where \mathbb{D} is the diagonal degree matrix, and ρ is the autocorrelation parameter – set as 1 for the intrinsic problems. Since this is the precision matrix, eigenvectors corresponding to the smallest non-zero eigenvalues of \mathbb{Q} capture smooth, large-scale spatial structure. We retain the first k eigenvectors (excluding the constant null vector), forming $\mathbf{Z}_{\text{ICAR}} \in \mathbb{R}^{n \times k}$.

Both bases provide orthogonal decompositions of spatial variation, as they are derived from eigenvectors of spatial covariance (MEM) or precision (ICAR) matrices. We set $k = 400$ based on residual spatial autocorrelation diagnostics (Moran’s I test, refer to Table 1). To avoid overfitting, we penalize the regression coefficients on these basis functions in the causal estimation procedure described below.

3.3 Doubly Robust Causal Estimation

To estimate the causal effect of each treatment on health outcomes in the presence of spatial confounding, we employ a doubly robust (DR) estimator based on the generalized propensity score (GPS) for continuous treatments [5].

The DR framework combines two nuisance functions:

- (i) **GPS estimation:** For the ℓ -th treatment, we model its conditional distribution given all other variables:

$$A_{\ell,j} \mid \mathbf{X}_j, \mathbf{A}_j^{-\ell}, \mathbf{Z}_j \sim N(\mu_\ell(\mathbf{X}_j, \mathbf{A}_j^{-\ell}, \mathbf{Z}_j), \sigma_\ell^2), \tag{2}$$

The conditional mean model μ_ℓ is estimated via a regularized regression with $A_{\ell,j}$ as the response and the remaining confounder set $(\mathbf{X}_j, \mathbf{A}_j^{-\ell}, \mathbf{Z}_j)$ as the predictor. Here we use an \mathcal{L}_1 penalty on spatial basis coefficients. Residual variance σ_ℓ^2 is estimated using the residual mean square error. Following that, the estimated GPS is given by the conditional normal density

$$f(A_{\ell,j} \mid \mathbf{X}_j, \mathbf{A}_j^{-\ell}, \mathbf{Z}_j) = \phi(A_{\ell,j}; \widehat{\mu}_\ell(\mathbf{X}_j, \mathbf{A}_j^{-\ell}, \mathbf{Z}_j), \widehat{\sigma}_\ell^2). \tag{3}$$

This leads to the construction of stabilized inverse probability weights [20, 28]:

$$w_{j\ell} = \frac{f(A_{\ell,j})}{f(A_{\ell,j} \mid \mathbf{X}_j, \mathbf{A}_j^{-\ell}, \mathbf{Z}_j)}, \tag{4}$$

where $f(A_{\ell,j})$ is the marginal density of the treatment $A_{\ell,j}$. We estimate it using the empirical distribution of $A_{\ell,j}$. This creates a pseudo-population where $A_{\ell,j}$ is balanced across confounders $\mathbf{X}_j, \mathbf{A}_j^{(-\ell)}$, and \mathbf{Z}_j . [20, 21]

- (ii) **Outcome model:** For the ℓ -th treatment, we model the outcome via a weighted likelihood function:

$$y_j \mid \mathbf{X}_j, A_{\ell,j}, \mathbf{A}_j^{-\ell}, \mathbf{Z}_j \sim N(g_{\ell,j}(\mathbf{X}_j, A_{\ell,j}, \mathbf{A}_j^{-\ell}, \mathbf{Z}_j), \zeta_\ell^2/w_{j\ell}), \quad (5)$$

where $g_{\ell,j}$ represents the conditional mean outcome and $w_{j\ell}$ are GPS weights from Equation (4). The mean model $g_{\ell,j}$ is fitted using a weighted regression model with y_j as the response, all the treatments and additional covariates $(\mathbf{X}_j, A_{\ell,j}, \mathbf{A}_j^{-\ell}, \mathbf{Z}_j)$ as the predictors, and the GPS weights $w_{j\ell}$ as the weight for the j -th observation. Again, the spatial basis coefficients are penalized in a similar way with an \mathcal{L}_1 penalty to avoid overfitting, leading to a lasso-type solutions for the coefficients. Coefficients on the other covariates are unpenalized to preserve causal interpretability.

The DR estimator for the marginal effect of treatment ℓ is:

$$\hat{\tau}_\ell = \frac{\partial \hat{g}_{\ell,j}}{\partial A_{\ell,j}} + \frac{1}{n} \sum_{j=1}^n w_{j\ell} \cdot \frac{(y_j - \hat{g}_{\ell,j})(A_{\ell,j} - \hat{\mu}_\ell)}{\hat{\zeta}_\ell^2}, \quad (6)$$

where the first term is the outcome model coefficient and the second term is a GPS-based bias correction. This estimator is consistent if *either* the GPS model 3 or the outcome model 5 is correctly specified [9]. Standard errors are computed via the empirical influence function:

$$\text{SE}(\hat{\tau}_\ell) = \sqrt{\frac{1}{n} \text{Var} \left(w_{j\ell} \cdot \frac{(y_j - \hat{g}_{\ell,j})(A_{\ell,j} - \hat{\mu}_\ell)}{\hat{\zeta}_\ell^2} \right)}. \quad (7)$$

We implement K -fold cross-fitting to control overfitting bias in the doubly robust estimator. Specifically, we partition the data into K mutually exclusive folds $\{\mathcal{I}_k\}$, $k = 1 \dots, K$. For each fold k , we treat \mathcal{I}_k as the held-out (test) set and use the remaining data \mathcal{I}_k^c as the training set. The procedure is as follows:

1. **GPS estimation:** For each fold k , using only the training data \mathcal{I}_k^c , estimate the GPS by fitting a Lasso regression with $A_{\ell,j}$ as the response and $(\mathbf{X}_j, \mathbf{A}_j^{-\ell}, \mathbf{Z}_j)$ as predictors. The penalty parameter $\lambda_{\text{GPS},\ell}$ is selected via cross-validation on the training data. We then obtain cross-fitted predictions $\hat{\mu}_{\ell,j}$ for all $j \in \mathcal{I}_k$. Repeating this over all folds yields $\hat{\mu}_{\ell,j}$ for all observations.
2. **Outcome model:** Similarly, for each fold k , we fit the outcome model using \mathcal{I}_k^c and obtain predictions on \mathcal{I}_k . The penalty parameter $\lambda_{\text{Outcome},\ell}$ is selected via cross-validation. For interpretability, only the spatial basis coefficients \mathbf{Z}_j are penalized in this step, while treatment and covariate effects remain unpenalized. This yields cross-fitted outcome predictions $\hat{g}_{\ell,j}$ for all j .

3. **DR Estimator:** Using the cross-fitted estimates $\{\widehat{\mu}_{j\ell}, \widehat{g}_{j\ell}\}_{j=1}^n$, we compute the doubly robust estimator as defined in Equation (6).

4 Results

Number of Bases (k)	Basis	RMSE (10^{-1})	MAE (10^{-1})	R^2	Active Bases Count	Moran's p -val
100	MEM	2.26	1.74	0.88	91	0.00
	ICAR	2.17	1.66	0.89	96	0.00
150	MEM	2.17	1.66	0.89	141	0.00
	ICAR	2.07	1.57	0.90	145	0.00
200	MEM	2.12	1.63	0.90	185	0.00
	ICAR	2.02	1.54	0.91	188	0.00
250	MEM	2.12	1.62	0.90	221	0.00
	ICAR	2.02	1.54	0.91	223	0.00
300	MEM	2.10	1.61	0.90	246	0.00
	ICAR	2.00	1.53	0.91	254	0.00
350	MEM	2.09	1.61	0.90	274	0.02
	ICAR	1.98	1.51	0.91	295	0.00
400	MEM	2.07	1.60	0.90	310	0.42
	ICAR	1.98	1.51	0.91	329	0.23
450	MEM	2.06	1.59	0.90	348	0.98
	ICAR	1.98	1.51	0.91	345	0.60
500	MEM	2.05	1.58	0.90	389	1.00
	ICAR	1.97	1.50	0.91	375	0.93

Table 1 Comparative performance of MEM and ICAR spatial bases across varying dimensions (k). Note the transition to non-significant Moran's I results ($p > 0.05$) at $k \geq 400$, indicating successful removal of residual spatial autocorrelation.

Table 2 Doubly robust causal effect estimates of all treatments

Treatment	Effect	SE	95% CI
Food Insecurity	0.086	0.004	[0.077, 0.094]
Unemployment Rate	5.190	0.614	[3.986, 6.393]
Pay Gap	0.160	0.071	[0.021, 0.300]
Rent Burden	0.110	0.099	[-0.085, 0.304]
Homeownership	-0.004	0.002	[-0.008, 0.000]
PM 2.5	0.000	0.004	[-0.008, 0.007]

Table 1 compares MEM and ICAR across basis dimensions $k \in \{100, 150, 200, \dots, 500\}$. ICAR marginally but consistently outperforms MEM on predictive accuracy across all values of k , and is therefore used in the causal estimation that follows. Both bases successfully eliminate residual spatial autocorrelation by $k = 400$ (Moran’s $I = 0.004$, $p = 0.334$), with prediction performance remaining stable beyond that point. We adopt $k = 400$ as the smallest basis dimension that achieves adequate spatial deconfounding.

Table 2 reports doubly robust GPS estimates for six socioeconomic and environmental determinants, all of which pass the residual autocorrelation check (Moran’s I , $p > 0.05$). Food insecurity and unemployment rate emerge as the dominant drivers of physical morbidity. A one percentage point increase in food insecurity corresponds to 0.086 additional unhealthy days per month, so a five point increase implies roughly 5.2 additional days per year. The unemployment rate effect is also similar in magnitude: a five point increase corresponds to approximately 3.1 additional unhealthy days per year. Pay gap carries a modest but statistically significant positive effect. Homeownership is borderline significant in the negative direction, plausibly reflecting its role as a broad proxy for household economic stability. Rent burden and PM 2.5 show no significant effects after spatial adjustment – a finding that may reflect weak marginal relationships at the county scale, attenuation from geographic aggregation, or both.

5 Discussion

This study applied a spatial causal inference framework combining basis function regularization with doubly robust GPS estimation to identify socioeconomic drivers of physical morbidity across U.S. counties. ICAR-derived eigenvectors marginally but consistently outperformed MEM in both prediction accuracy and residual autocorrelation removal. Among the six treatments examined, food insecurity and unemployment rate are the dominant causal drivers of physically unhealthy days, with pay gap modestly significant and homeownership borderline negative. Rent burden and PM 2.5 show no significant effects after spatial adjustment, plausibly reflecting attenuation from county-level aggregation or mediation through other pathways.

Several limitations warrant consideration. The data are cross-sectional and county-level, limiting causal direction and introducing ecological fallacy concerns only based on the current version of the data. Basis dimension selection also presents a fundamental problem: standard information criteria (AIC, BIC, DIC) and residual autocorrelation diagnostics do not usually agree here. Our chosen $k = 400$ prioritizes the elimination of spatial dependence over model simplicity, and we acknowledge that a full-rank ICAR or Gaussian Process models could provide a more theoretically complete (albeit computationally intensive) alternative. It should be noted though that prediction performance has remained competitive throughout.

Future research should extend this framework into a spatiotemporal formulation. Utilizing multiple releases of CHR&R data would allow for the exploitation of within-county variation over time, specifically to test the stability of unemployment and food insecurity effects across major shocks like the COVID-19 pandemic. Additionally, more health-related outcomes such as mentally unhealthy days, or even a multivariate

framework modeling physical and mental health outcomes jointly would likely yield a more holistic understanding of how structural disadvantage shapes the American health landscape.

Declarations

The authors report no external funding and no competing interests. All data used in this study are publicly available from the 2022 County Health Rankings & Roadmaps (<https://www.countyhealthrankings.org>) and the U.S. Census Bureau American Community Survey 5-year estimates <https://data.census.gov>. All authors contributed equally to this work.

References

- [1] Braveman, P., Egerter, S., Williams, D.R.: The social determinants of health: coming of age. *Annual review of public health* **32**(1), 381–398 (2011)
- [2] Remington, P.L.: County health rankings and the cult of the imperfect. *Health Services Research* **50**(5), 1407 (2015)
- [3] Clayton, D.G., Bernardinelli, L., Montomoli, C.: Spatial correlation in ecological analysis. *International journal of epidemiology* **22**(6), 1193–1202 (1993)
- [4] Paciorek, C.J.: The importance of scale for spatial-confounding bias and precision of spatial regression estimators. *Statistical science: a review journal of the Institute of Mathematical Statistics* **25**(1), 107 (2010)
- [5] Hirano, K., Imbens, G.W.: 7. The Propensity Score with Continuous Treatments, pp. 73–84. John Wiley & Sons, Ltd, ??? (2004). <https://doi.org/10.1002/0470090456.ch7>
- [6] Giffin, A., Reich, B., Yang, S., Rappold, A.: Generalized propensity score approach to causal inference with spatial interference. *Biometrics* **79**(3), 2220–2231 (2023)
- [7] Cressie, N., Sainsbury-Dale, M., Zammit-Mangion, A.: Basis-function models in spatial statistics. *Annual Review of Statistics and Its Application* **9**, 373–400 (2022)
- [8] Hooten, M.B., Ver Hoef, J.M., Hanks, E.M.: Simultaneous autoregressive (sar) model. *Wiley StatsRef: Statistics Reference Online*, 1–10 (2014)
- [9] Kennedy, E.H., Ma, Z., McHugh, M.D., Small, D.S.: Non-parametric methods for doubly robust estimation of continuous treatment effects. *Journal of the Royal Statistical Society Series B: Statistical Methodology* **79**(4), 1229–1245 (2017)

- [10] Shiba, K., Kawahara, T.: Using propensity scores for causal inference: pitfalls and tips. *Journal of epidemiology* **31**(8), 457–463 (2021)
- [11] Reich, B.J., Yang, S., Guan, Y., Giffin, A.B., Miller, M.J., Rappold, A.: A review of spatial causal inference methods for environmental and epidemiological applications. *International Statistical Review* **89**(3), 605–634 (2021)
- [12] Rivera, K.M., Mollalo, A., et al.: Spatial analysis and modelling of depression relative to social vulnerability index across the united states. *Geospatial health* **17**(2) (2022)
- [13] Comas, C., Martínez, A., Blanch, A.: Self-reported mental distress in the united states: a bayesian analysis of the spatial structure over the covid-19 pandemic across age groups. *International Journal of Health Geographics* **24**(1), 30 (2025)
- [14] Hodges, J.S., Reich, B.J.: Adding spatially-correlated errors can mess up the fixed effect you love. *The American Statistician* **64**(4), 325–334 (2010)
- [15] Hanks, E.M., Schliep, E.M., Hooten, M.B., Hoeting, J.A.: Restricted spatial regression in practice: geostatistical models, confounding, and robustness under model misspecification. *Environmetrics* **26**(4), 243–254 (2015)
- [16] Griffith, D., Chun, Y.: Spatial autocorrelation and spatial filtering. *Handbook of regional science* **1**, 1477–1507 (2014)
- [17] Dray, S., Legendre, P., Peres-Neto, P.R.: Spatial modelling: a comprehensive framework for principal coordinate analysis of neighbour matrices (pcnm). *Ecological modelling* **196**(3-4), 483–493 (2006)
- [18] Besag, J., York, J., Mollié, A.: Bayesian image restoration, with two applications in spatial statistics. *Annals of the institute of statistical mathematics* **43**(1), 1–20 (1991)
- [19] Hughes, J., Haran, M.: Dimension reduction and alleviation of confounding for spatial generalized linear mixed models. *Journal of the Royal Statistical Society Series B: Statistical Methodology* **75**(1), 139–159 (2013)
- [20] Robins, J.M., Hernan, M.A., Brumback, B.: *Marginal structural models and causal inference in epidemiology*. Lww (2000)
- [21] Hernán, M.A., Robins, J.M.: *Causal Inference*. CRC Boca Raton, FL, ??? (2010)
- [22] Robins, J.M., Rotnitzky, A.: Comment on the bickel and kwon article, “inference for semiparametric models: Some questions and an answer”. *Statistica Sinica* **11**(4), 920–936 (2001)
- [23] Funk, M.J., Westreich, D., Wiesen, C., Stürmer, T., Brookhart, M.A., Davidian, M.: Doubly robust estimation of causal effects. *American journal of epidemiology*

173(7), 761–767 (2011)

- [24] Gao, B., Wang, J., Stein, A., Chen, Z.: Causal inference in spatial statistics. *Spatial statistics* **50**, 100621 (2022)
- [25] Papadogeorgou, G., Samanta, S.: Spatial causal inference in the presence of unmeasured confounding and interference. arXiv preprint arXiv:2303.08218 (2023)
- [26] Pollmann, M.: Causal inference for spatial treatments. arXiv preprint arXiv:2011.00373 (2020)
- [27] Griffith, D.A.: Interpreting moran eigenvector maps with the getis-ord g_i^* statistic. *The Professional Geographer* **73**(3), 447–463 (2021)
- [28] Naimi, A.I., Moodie, E.E., Auger, N., Kaufman, J.S.: Constructing inverse probability weights for continuous exposures: a comparison of methods. *Epidemiology* **25**(2), 292–299 (2014)